EUROPEAN UROLOGY FOCUS 6 (2020) 1205–1212

available at www.sciencedirect.com
journal homepage: www.europeanurology.com/eufocus

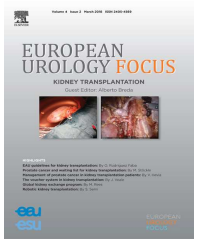

Prostate Cancer

Combined Clinical Parameters and Multiparametric Magnetic Resonance Imaging for the Prediction of Extraprostatic Disease—A Risk Model for Patient-tailored Risk Stratification When Planning Radical Prostatectomy

Joanne Nyarangi-Dix[a], *Manuel Wiesenfarth*[b], *David Bonekamp*[c], *Bertram Hitthaler*[a], *Viktoria Schütz*[a], *Svenja Dieffenbacher*[a,b], *Maya Mueller-Wolf*[c], *Wilfried Roth*[d,1], *Albrecht Stenzinger*[d], *Stefan Duensing*[a], *Matthias Roethke*[c], *Dogu Teber*[a,2], *Heinz-Peter Schlemmer*[c], *Markus Hohenfellner*[a], *Jan Philipp Radtke*[a,c,*]

[a] *Department of Urology, University Hospital Heidelberg, Heidelberg, Germany;* [b] *Division of Biostatistics, German Cancer Research Center (DKFZ), Heidelberg, Germany;* [c] *Department of Radiology, German Cancer Research Center (DKFZ), Heidelberg, Germany;* [d] *Institute of Pathology Heidelberg, Ruprecht-Karls-University Heidelberg, Heidelberg, Germany*

Article info

Article history:
Accepted November 10, 2018

Associate Editor: Derya Tilki

Keywords:
Prostate cancer
Magnetic resonance imaging
Risk model
Nomogram
Extraprostatic extension
Radical prostatectomy

Abstract

Background: Multiparametric magnetic resonance imaging (mpMRI) facilitates the detection of significant prostate cancer. Therefore, addition of mpMRI to clinical parameters might improve the prediction of extraprostatic extension (EPE) in radical prostatectomy (RP) specimens.
Objective: To investigate the accuracy of a novel risk model (RM) combining clinical and mpMRI parameters to predict EPE in RP specimens.
Design, setting, and participants: We added prebiopsy mpMRI to clinical parameters and developed an RM to predict individual side-specific EPE (EPE-RM). Clinical parameters of 264 consecutive men with mpMRI prior to MRI/transrectal ultrasound fusion biopsy and subsequent RP between 2012 and 2015 were retrospectively analysed.
Outcome measurements and statistical analysis: Multivariate regression analyses were used to determine significant EPE predictors for RM development. The prediction performance of the novel EPE-RM was compared with clinical T stage (cT), MR–European Society of Urogenital Radiology (ESUR) classification for EPE, two established nomograms (by Steuber et al and Ohori et al) and a clinical nomogram based on the coefficients of the established nomograms, and was constructed based on the data of the present cohort, using receiver operating characteristics (ROCs). For comparison, models' likelihood ratio (LR) tests and Vuong tests were used. Discrimination and calibration of the EPE-RM were validated based on resampling methods using bootstrapping.
Results and limitations: International society of Urogenital Pathology grade on biopsy, ESUR criteria, prostate-specific antigen, cT, prostate volume, and capsule contact length were included in the EPE-RM. Calibration of the EPE-RM was good (error 0.018). The ROC

[1] Current affiliation: Institute of Pathology, Mainz University Medical Center, Mainz, Germany.
[2] Current affiliation: Department of Urology, Städtisches Klinikum Karlsruhe, Karlsruhe, Germany.
[*] Corresponding author. Department of Urology, Ruprecht-Karls-Universität Heidelberg, Im Neuenheimer Feld 110, 69120 Heidelberg, Germany. Tel.: +49 6221 56 36454; Fax: +49 6221 56 5366.
E-mail address: j.radtke@dkfz-heidelberg.de (J.P. Radtke).

https://doi.org/10.1016/j.euf.2018.11.004

area under the curve for the EPE-RM was larger (0.87) compared with cT (0.66), Memorial Sloan Kettering Cancer Center nomogram (0.73), Steuber nomogram (0.70), novel clinical nomogram (0.79), and ESUR classification (0.81). Based on LR and Vuong tests, the EPE-RM's model fit was significantly better than that of cT, all clinical models, and ESUR classification alone ($p < 0.001$). Limitations include monocentric design and expert reading of MRI.

Conclusions: This novel EPE-RM, incorporating clinical and MRI parameters, performed better than contemporary clinical RMs and MRI predictors, therefore providing an accurate patient-tailored preoperative risk stratification of side-specific EPE.

Patient summary: Extraprostatic extension of prostate cancer can be predicted accurately using a combination of magnetic resonance imaging and clinical parameters. This novel risk model outperforms magnetic resonance imaging and clinical predictors alone and can be useful when planning nerve-sparing radical prostatectomy.

1. Introduction

Accurate prediction of extraprostatic extension (EPE) in prostate cancer (PC) is useful when planning radical prostatectomy (RP) and estimating a patient's prognosis [1,2]. Local staging is traditionally based on clinical parameters, such as prostate-specific antigen (PSA) and clinical T stage (cT) on digital rectal examination (DRE). However, their predictive power is currently unclear [3,4]. Several nomograms, for example, the Partin tables, apply combined clinical parameters for EPE prediction [5–7]. Despite external validation of the Partin tables, the use of elder histopathological classifications as well as missing specifications of side-specific prostatic tumour involvement raises substantial challenges.

To improve current risk predictors, Steuber et al [6] developed a nomogram for side-specific EPE prediction using clinical data [8]. Another nomogram for the prediction of side-specific EPE probability was published by Ohori et al [7] from the Memorial Sloan Kettering Cancer Center (MSKCC).

Multiparametric magnetic resonance imaging (mpMRI) of the prostate, which is increasingly being performed prior to targeted prostate biopsy when PC is suspected, can be useful in the detection of EPE [1,9–12]. In addition, preoperative mpMRI can significantly increase the predictive value of clinical parameters [12]. A meta-analysis on mpMRI showed limited sensitivity of 57% for EPE detection, but 90% specificity [13]. Within the European Society of Urogenital Radiology (ESUR) guidelines, criteria (ESUR classification) have been defined for EPE, seminal vesicle (SV) invasion, involvement of the bladder neck, and pelvic floor muscle (PFM) [9]. Standardised assessment based on these ESUR classifications increases the precision to predict EPE [14–16]. Rayn et al [17] recently combined MRI and MSKCC nomogram, demonstrating a benefit of adding MRI to clinical parameters in EPE prediction.

Therefore, the purpose of our study was to develop a risk model (RM) for the prediction of EPE (EPE-RM) by combining clinical and MRI parameters. Furthermore, we sought to compare the novel EPE-RM with cT, a novel clinical nomogram developed using the parameters of the Steuber and MSKCC nomograms, the established Steuber and MSKCC nomograms, and ESUR classification alone.

2. Patients and methods

2.1. Patient cohort

Institutional review board approval was obtained (S011/2011), and all participants provided written informed consent. All men were enrolled and registered into a prospective database assessing MRI-targeted/transrectal ultrasound (TRUS) fusion biopsy between 2015 and 2016. PSA screening was not performed in a structured manner. Subgroups of this cohort were previously reported [11,15,18].

Inclusion criteria were mpMRI in accordance with the Prostate Imaging Reporting and Data System (PI-RADS) guidelines prior to MRI/TRUS fusion biopsy, positive evidence of PC in biopsy, and an indication to undergo RP in our department based on recent guidelines [9].

The cohort consisted of 264 retrospectively analysed consecutive men with complete data on biopsy outcome, PSA, age, DRE, prostate volume (PV), PSA density, RP outcome, including T stage, EPE, and tumour volume (TV). In addition, data on PI-RADSv2.0 of every lesion called by radiologists (in particular, the index lesion), ESUR classification, capsule contact length (CCL), TV and diameter of the lesion on MRI, and localisation (side/hemisphere) were available [19]. These samples served for EPE-RM development, internal validation and comparisons with ESUR classification, cT, the Steuber and MSKCC nomograms, a new calibrated model in our cohort including the parameters of the established clinical nomograms, and a combination of this clinical model + MRI [6,7,9].

2.2. Imaging

All MR images were acquired according to the ESUR guidelines at two 3-Tesla scanners (Magnetom Prisma and Biograph mMR, Siemens Healthcare, Erlangen, Germany; Supplementary Table 1) [9].

Image analyses were prospectively performed according to PI-RADSv2.0 by or under the supervision of three expert uroradiologists (H.P.S., M.C.R., and D.B. with 18, 8, and 10 yr of experience in prostate MRI, respectively) [19].

PV, CCL, lesion diameter, and volume were retrospectively determined using high-resolution T2 w sequences with ITK-SNAP software (www.itk-snap.org). ESUR classification for EPE includes dedicated criteria for assessing extraprostatic tumour extension, SV invasion, and involvement of the bladder neck and PFM, determined by the above-mentioned uroradiologists [9].

2.3. MRI/TRUS fusion biopsy

All men underwent transperineal MRI fusion targeted biopsies of MRI-suspicious lesions first (two to five cores, median two per lesion) and then transperineally conducted systematic biopsies (SBs; median 24 cores) [11,18].

2.4. Surgical technique

A total of 176 men (67%) underwent robot-assisted RP and 88 (33%) retropubic RP in our department. Each RP was performed by one of five experienced surgeons, each with at least 4 yr of experience, having performed >100 RPs. The surgeon was aware of the MRI results. However, a regular preoperative radiological presentation of the MRI was not performed.

2.5. Pathological workup

Histopathological analyses were performed under the supervision of one dedicated uropathologist (W.R., 15-yr experience) according to the International Society of Urological Pathology (ISUP) standards.

2.6. Nomogram calculation

The likelihood of EPE according to the Steuber and MSKCC nomograms was retrospectively determined using the original nomograms [6,7]. For the MSKCC nomogram, the full model was used and calculated manually, as the coefficients have not been published [7]. For the new clinical model, we used ISUP grade, cT, PSA, core involvement in %, and percentage of positive cores, and fitted a clinical model based on our cohort. Last, we added MRI information on the new clinical model (clinical model + MRI).

2.7. Statistical analysis

Patient, MRI, biopsy, and RP data were analysed descriptively (Table 1). First, we performed a multivariate logistic regression analysis to predict the presence of EPE in RP specimens. Regression-based coefficients were used for a full model, which included all tested coefficients, and for EPE-RM development (Fig. 1).

Development was performed by backward variable selection based on Akaike's information criterion (AIC). Bootstrapped feature selection frequencies are given in Supplementary Table 2.

Discrimination of cT, ESUR MRI classification, the published Steuber and MSKCC nomograms, the novel clinical model, the novel clinical model + MRI, the novel full model, and the EPE-RM were compared using the area under the curve (AUC) of receiver-operating-characteristic (ROC) curve analysis with internal validation by bootstrapping with 1000 iterations (Fig. 2; for details see the Supplementary material, Information on internal validation using bootstrapping).

LR test was used for a comparison of nested models; otherwise, Vuong test for comparing non-nested models was performed (Table 2) [20].

The extent of over- or underestimation of predicted probabilities relative to observed probabilities of PC was explored by a calibration plot, which was internally validated using bootstrapping with 1000 iterations (Fig. 3).

All performed tests were two sided, with a significance level of 5%.

Statistical analyses were performed using R version 3.5.0 (R Foundation for Statistical Computing, Vienna, Austria). Reporting followed the Standards of Reporting of Diagnostic Accuracy (Supplementary Table 3).

Table 1 – Patient cohort with clinical, MRI, surgical, and histological parameters.

Patients cohort	
Patients (no.)	264
Median age, yr (IQR)	65 (60; 70)
Median PSA level, ng/ml (IQR)	8.2 (5.9; 13.0)
Suspicious digital rectal examination (≥cT2), no. (%)	55 (21)
Median prostate volume, ml (IQR)	39 (30; 51)
Men with previous prostate biopsy, no. (%)	163 (62)
Men without previous prostate biopsy, no. (%)	101 (38)
Median PSA density, ng/ml/ml (IQR)	0.22 (0.17; 0.28)
Men with PI-RADS 3–5 lesions on mpMRI, no. (%)	233 (88.3)
Number of PI-RADS lesions and median per patient (IQR)	285; 1 (1–2)
Median ESUR classification of EPE sum score (IQR)	5 (4; 7)
Median capsule contact length, mm (IQR)	13 (7; 20)
Median lesion volume, ml (IQR)	1.3 (0.8; 2.8)
Biopsies per patient, median (IQR)	28 (25–30)
Systematic biopsies per patient, median (IQR)	24 (22–25)
Targeted biopsies per patient, median (IQR)	4 (3; 5)
Risk groups according to the National Comprehensive Cancer Network	
Low risk, no. (%)	34 (13)
Intermediate risk, no. (%)	153 (58)
High risk, no. (%)	77 (29)
Median time from biopsy to RP, d (IQR)	56 (42–70)
Retropubic open radical prostatectomy, no. (%)	88 (33)
DaVinci-assisted robotic radical prostatectomy, no. (%)	176 (67)
Nerve-sparing radical prostatectomy, no. (%)	191 (72)
T stage, no. (%)	
pT2	136 (52)
pT3a	81 (31)
pT3b	43 (16)
pT4	4 (2)
Patients with EPE in RP specimen	127 (48)
Side-specific EPE in RP specimen—prostate hemispheres with EPE, no. (%)	218 (41)
ISUP grade 1	17 (7)
ISUP grade 2	143 (54)
ISUP grade 3	64 (24)
ISUP grade 4	8 (3)
ISUP grade 5	32 (12)
Nodal status, no. (%)	
N0	221 (84)
N+	43 (16)
Surgical margin status	
R0, no. (%)	212 (80)
R1, no. (%)	52 (20)
R1 in pT2, no. (% of all pT2)	16 (12)
R1 in pT3/4, no. (% of all pT3/4)	36 (28)

cT = clinical T stage; EPE = extraprostatic extension; ESUR = European Society of Urogenital Radiology; IQR = interquartile range; ISUP = International Society of Urogenital Pathology; MRI = magnetic resonance Imaging; mpMRI = multiparametric magnetic resonance Imaging; PI-RADS = Prostate Imaging Reporting and Data System; PSA = prostate-specific antigen; RP = radical prostatectomy.

3. Results

Patient demographics, MRI, biopsy, and RP data are given in Table 1. In summary, 48% of patients and 41% of prostate hemispheres had an EPE in the RP specimen.

After stepwise backward elimination of variables from the full model based on AIC, lesion diameter, core involvement in %, percentage of positive cores, and PI-RADSv2.0 were omitted from the final EPE-RM, with bootstrap feature selection frequencies as low as 14%, 7.7%, 7.0%, and 6.8%, respectively (Supplementary Table 3). Accordingly, ISUP grade, PV on MRI, ESUR classification, PSA level, cT, and CCL were considered relevant to the EPE-RM (Table 3 and Fig. 1). Inclusion of the lesion diameter, core involvement in %, percentage of positive cores, and PI-RADSv2.0 in the EPE-RM did not improve discrimination, as apparent in Fig. 2.

On ROC curve analyses (Fig. 2 and Table 2), the EPE-RM, full model, and novel clinical model + MRI reached almost identical AUCs (0.86, 0.86, and 0.85, respectively), all being higher compared with the ESUR classification for EPE (0.81),

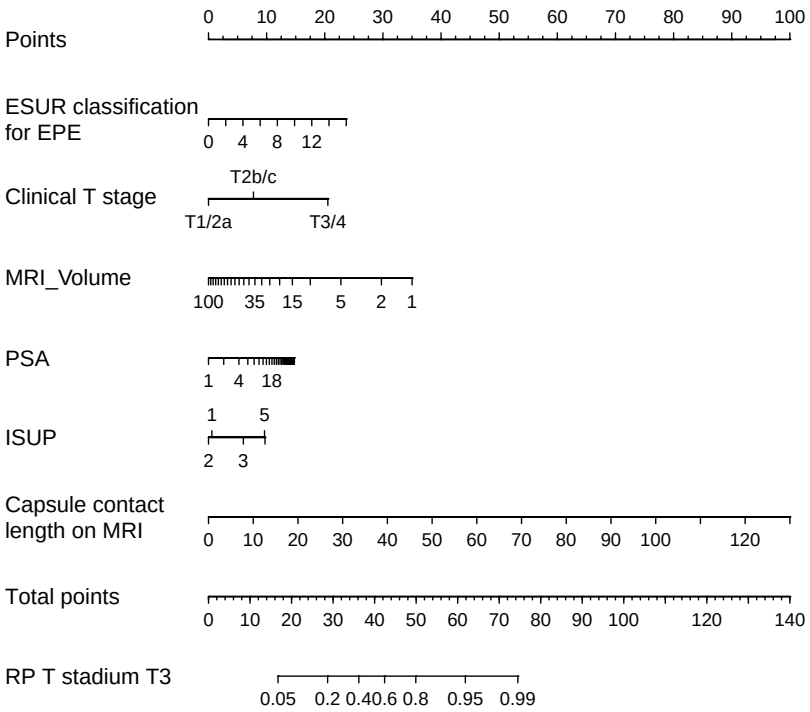

Fig. 1 – EPE-RM derived from parameters: DRE, PSA, ISUP grade in biopsy, MRI volume, ESUR classification, and capsule contact length. DRE = digital rectal examination; EPE-RM = risk model for the prediction of extraprostatic extension; ESUR = European Society of Urogenital Radiology; ISUP = International society of Urogenital Pathology; MRI = magnetic resonance imaging; PSA = prostate-specific antigen; RP = radical prostatectomy.

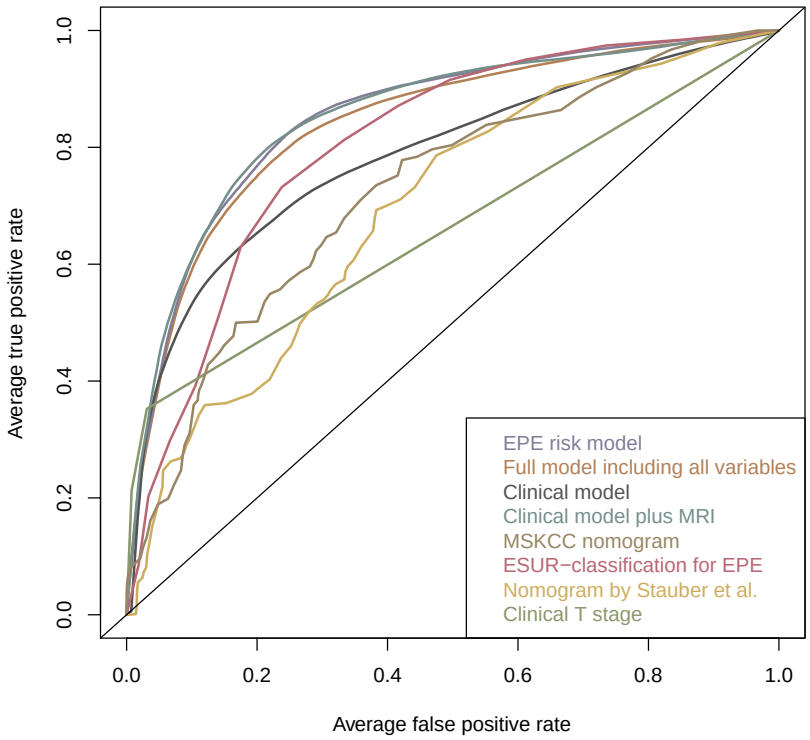

Fig. 2 – ROC curve analysis of the EPE-RM (blue), the full model (orange), the nomograms published by Ohori et al (MSKCC nomogram, brown) and Steuber et al (yellow), the novel clinical model (dark green), clinical model + MRI (turquoise), ESUR classification (pink), and clinical T stage (bright green) for the prediction of an EPE. AUCs are given in Table 3. AUC = area under the curve; EPE = extraprostatic extension; EPE-RM = risk model for the prediction of EPE; ESUR = European Society of Urogenital Radiology; MRI = magnetic resonance imaging; MSKCC = Memorial Sloan Kettering Cancer Center.

Table 2 – AUC in ROC curve analysis for the EPE-RM, the full model including all variables, the ESUR MRI classification for EPE, clinical T stage, the established clinical nomograms by Steuber et al and MSKCC, the clinical model and clinical model + MRI, and comparisons of models using LR and Vuong tests.

Parameter	
Prediction model/parameter	**AUC in ROC curve analysis**
EPE risk model	0.86
Full model including all variables	0.86
cT	0.66
ESUR MRI classification for EPE	0.81
Nomogram by Steuber et al	0.70
MSKCC nomogram	0.73
Clinical model	0.79
Clinical model + MRI	0.85
Comparison of models for side-specific EPE using LR test	**pvalue**
EPE risk model vs ESUR MRI classification for EPE	<0.001
EPE risk model vs cT	<0.001
Clinical model vs clinical model + MRI	<0.001
Comparison of models for side-specific EPE using Vuong test	**pvalue**
EPE risk model vs nomogram by Steuber et al	<0.001
EPE risk model vs MSKCC nomogram	<0.001
EPE risk model vs clinical model	<0.001
EPE risk model vs clinical model + MRI	0.89

AUC = area under the curve; cT = clinical T stage; EPE = extraprostatic extension; EPE-RM = risk model for the prediction of EPE; ESUR = European Society of Urogenital Radiology; LR = likelihood ratio; MRI = magnetic resonance imaging; MSKCC = Memorial Sloan Kettering Cancer Center; ROC = receiver operating characteristics.

cT (0.66), the published Steuber (0.70) and MSKCC (0.73) nomograms, and the novel clinical model (0.79) [6,7,9].

LR and Vuong test results showed that the EPE-RM performed significantly better compared with the ESUR classification, cT, the two established nomograms, and the novel clinical model ($p < 0.001$ each) based on a Bonferroni-adjusted threshold of 0.008 given a global significance level of 5%, while its performance was barely distinguishable from that of the clinical model +MRI ($p = 0.89$; Table 2).

The bootstrapped calibration plot of the EPE-RM (Fig. 3) demonstrates that there are no untoward deviations of predicted risk of EPE from the observed risk in the RP specimen over the entire range.

4. Discussion

The novel EPE-RM is one of the first approaches combining mpMRI and clinical parameters for a side-specific prediction of EPE in RP specimens. Rayn et al [17] recently demonstrated a higher predictive value for EPE when MRI is added to the MSKCC nomogram. Martini et al [21] constructed another nomogram including PSA, Gleason grade, core involvement in %, and absence or presence of EPE on MRI, which showed good discrimination with an AUC of 0.82. Reliability and improved discrimination of the present EPE-RM were influenced by several issues that are to be discussed below.

In our cohort, ISUP grade was a significant contributor to regression analysis. This is in contrast to the MSKCC and Steuber nomograms using Gleason score [6–8]. In our cohort, the incidence of EPE was lower for the 43 men with ISUP grade 1 in biopsy specimens (28%, not given in the results), compared with the 112 men with ISUP grade 2 PC (34%). However, in multivariate RM development, the nomogram was not monotonic in ISUP (odds ratio for ISUP 2 vs ISUP 1 was <1 [0.8], with a huge confidence interval [0.28–2.30] including odds ratios >1) due to collinearities. Therefore, we combined ISUP 1 and 2. Moreover, we combined ISUP 4 and 5 to improve stability because of relatively few cases in ISUP 4 and because their effects were almost identical. We acknowledge that this is not in accordance with recent literature [22,23].

For EPE prediction, utilisation of PSA and PSA density is controversial. Horiguchi et al [24] proved PSA density to be superior to PSA value. However, including both PV and PSA density into the model is likely to lead to collinearity issues and counterintuitive nomograms. It is important to note that the use of logarithmic PSA density is a special case by which logarithmic PSA plus logarithmic PV are applied when the regression coefficients of the latter two are fixed to be equal. Thus, incorporating log PSA and log PV instead of log PSA density can be considered as favourable. This is in line with previously published nomograms [6,7].

The proportion of positive cores and tumorous core involvement in % are often incorporated to predict the potential tumour extension and EPE. Martini et al [21] found that core involvement was a significant EPE predictor. In our cohort, both proportion of positive cores and tumorous core involvement in % were selected only in 7% and 7.7% of cases.

Table 3 – Multivariate logistical regression analysis for prediction of an EPE in RP specimen.

Parameter	Odds ratio	95% confidence interval	*p* value
ISUP grade			0.13
ISUP grade 3 vs 1/2	2.19	0.87–5.53	
ISUP grade 4/5 vs 1/2	3.52	1.00–12.37	
ESUR classification for EPE	2.17	1.11–4.22	0.02
PSA per ng/ml	1.45	0.90–2.35	0.13
Prostate volume on MRI	0.60	0.39–0.92	0.02
Clinical T stage			0.03
Clinical T-stage cT2b/c vs cT1/2a	2.74	0.60–12.66	
Clinical T-stage cT3/4 vs cT1/2a	14.59	1.70–125.33	
Capsule contact length on MRI	3.69	1.97–6.91	<0.001

cT = clinical T stage; EPE = extraprostatic extension; ESUR = European Society of Urogenital Radiology; ISUP = International Society of Urogenital Pathology; MRI = magnetic resonance Imaging; PSA = prostate-specific antigen; RP = radical prostatectomy.

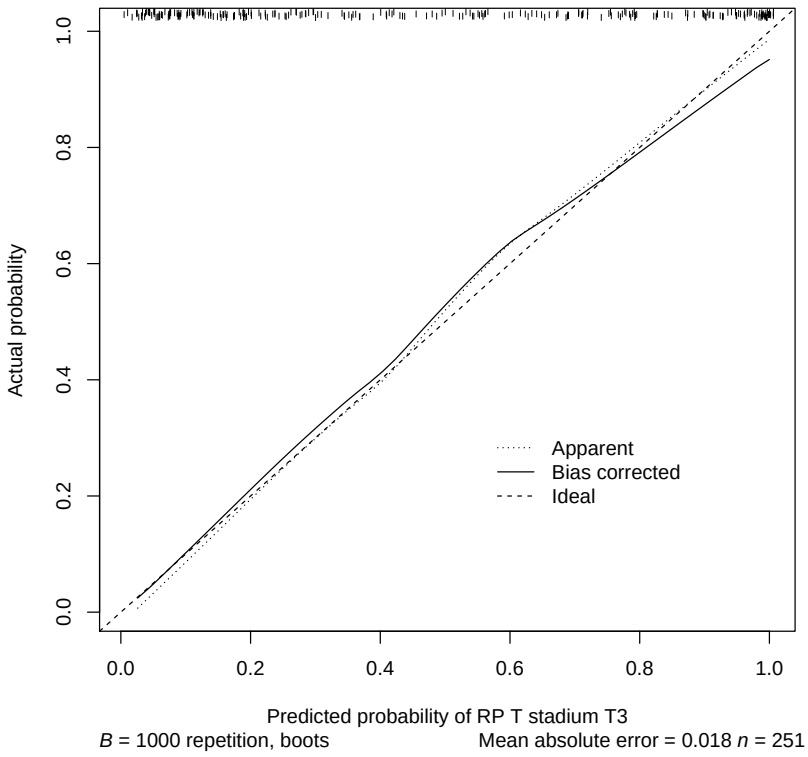

Fig. 3 – Calibration curve for the EPE-RM for predicting an EPE. The *x* axis shows the predicted likelihoods of the RM and the *y* axis shows the actual likelihoods. The dashed line indicates a perfect prediction, and the dotted line indicates the predicted versus actual EPE in the RM. The lines along the *x* axis show the number of patients with EPE. The mean absolute error of 0.018 reflects that the predicted and the actual values are closely correlated. EPE = extraprostatic extension; EPE-RM = risk model for the prediction of EPE; RM = risk model; RP = radical prostatectomy.

Inclusion of these two parameters in the EPE-RM did not demonstrate a benefit. Consequently, these two parameters were not included, in order to develop a reliable and pragmatic easy-to-use model.

The quality of MRI for EPE prediction depends on the experience and specialisation of the radiologist, and hence varies greatly [25–27]. Thus, it is important to define tangible parameters in order to increase the prediction value and allow reproducibility of an RM. The novel EPE-RM therefore integrated CCL into MRI and the standardised ESUR classification as predictors of EPE. Baco et al [28] demonstrated that the CCL on MRI can predict EPE accurately. The ESUR classification has repeatedly been validated, is reliable for EPE prediction with AUC values up to 0.86, and may attenuate the low sensitivity of MRI [14–16]. AUC of the standardised MRI reading was lower in the present analysis (0.81) compared with that of Boesen et al (0.86) [14], but higher compared with non-standardised reading (0.71) [12]. Since both applied MR parameters are easy to measure in a standard MRI setting hereby minimising interobserver variability, they are deemed reliable.

AUCs of the novel EPE-RM and clinical model + MRI parameters were higher, compared with the established and the novel clinical model (Fig. 2) [6,7]. These results may be due to inclusion of MRI parameters. This is supported by the increased prognostic value of both the ESUR classification (AUC 0.81) and the clinical model + MRI parameters (AUC 0.85) when compared with clinical nomograms [9]. In addition, Rayn et al [17] recently demonstrated significant improvement of the prediction value by inclusion of MRI parameters in the MSKCC nomogram. The additional benefit of adding MRI to clinical parameters within the EPE-RM and clinical model + MRI was comparable with that in the study of Rayn et al [17]. However, this benefit was due to ESUR classification and CCL on MRI, but not due to PI-RADS scoring. Interestingly, the improvement achieved by adding MRI parameters to an established clinical model is less in men who receive both targeted biopsy and SB, compared with men who receive only standard SB [17]. As all men in our cohort underwent fusion biopsy with targeted biopsy and SB, the use of our EPE-RM in a cohort of 12-core TRUS-biopsied men may result in further improvement compared with clinical parameters alone [17]. However, the performance of ESUR classification alone was good with an AUC of 0.81, thus being only slightly inferior to EPE-RM.

An additional value of the present EPE-RM is the individualised and side-specific risk assessment of EPE. This may be important when planning RP. With information derived from the EPE-RM (a side-specific, nerve-sparing approach), as well as appropriate intraoperative frozen sectioning or NeuroSAFE, can be planned in order to reduce the rate of positive surgical margins [29,30].

Our study has limitations. Transferability to other populations may be limited by the high prevalence of EPE (48%) in our cohort as far as the magnitude of predicted probabilities for individuals is concerned [6,7]. If the novel EPE-RM is applied to populations with lower prevalences, miscalibration will occur; that is, predicted probabilities will be overestimated (while discrimination performance will remain the same). Therefore, the EPE-RM model has to be recalibrated accordingly. However, this is a general dilemma faced by all RMs when the prevalence between development and validation cohort differs.

Since the advantage of PI-RADSv2.0 over PI-RADSv1.0 in detecting EPE remains unclear, use of version 2.0 is debatable. However, PI-RADSv2.0 has become the standard approach for MR reading of suspicious lesions [19]. In addition, all our mpMRI findings were studied by expert radiologists, which may limit their generalisability to cohorts for which expert reading is not available. We did not assess for interobserver variability for both PI-RADS and ESUR classification, as Rosenkrantz et al [31] did for PI-RADSv1.0. These points have to be contemplated when applying or validating our EPE-RM externally.

Cost-effectiveness has also to be discussed. For this study, all MRI findings had been performed for the MRI/TRUS fusion biopsy, and cost effectiveness of diagnostic MRI has been suggested recently [32].

As mentioned, all men in our cohort underwent transperineal MRI/TRUS fusion biopsy prior to RP. This may obviously limit the eligibility, when adopting the EPE-RM for cohorts with 12-core TRUS-biopsied men. As our study is lacking a comparison of EPE-RM performance for 12-core TRUS- versus fusion-biopsied patients, we cannot validate recent findings that the added value of mpMRI to clinical parameter models increases on cohorts with SB alone [17]. However, both Rayn et al [17] and Martini et al [21] state that the performance of models incorporating clinical and MRI findings decreases slightly, when applied to standard SB cohorts. Thus, our model's performance might decrease, but as external validation cohort is lacking, performance of our novel EPE-RM has not yet been validated in an independent population, men with 12-core TRUS SB, or a PSA-screened cohort.

5. Conclusions

The EPE-RM combining MRI and clinical parameters for the prediction of side-specific extraprostatic disease performed significantly better than RMs based on clinical and MRI parameters alone, previously published clinical nomograms, and a clinical parameter model.

Using this novel EPE-RM, the individual side-specific risk of EPE can be predicted well. This can be useful when counselling patients as well as during planning and performance of RP.

Author contributions: Jan Philipp Radtke had full access to all the data in the study and takes responsibility for the integrity of the data and the accuracy of the data analysis.

Study concept and design: Radtke.
Acquisition of data: Nyarangi-Dix, Radtke, Hitthaler, Schütz, Dieffenbacher, Roth, Stenzinger.
Analysis and interpretation of data: Wiesenfarth, Nyarangi-Dix, Radtke, Bonekamp, Mueller-Wolf.
Drafting of the manuscript: Radtke.
Critical revision of the manuscript for important intellectual content: Duensing, Schlemmer, Hohenfellner, Roethke.
Statistical analysis: Bonekamp, Radtke, Wiesenfarth.
Obtaining funding: None.
Administrative, technical, or material support: Roethke, Stenzinger, Radtke, Nyarangi-Dix.
Supervision: Hohenfellner, Radtke.
Other: None.

Financial disclosures: Jan Philipp Radtke certifies that all conflicts of interest, including specific financial interests and relationships and affiliations relevant to the subject matter or materials discussed in the manuscript (eg, employment/affiliation, grants or funding, consultancies, honoraria, stock ownership or options, expert testimony, royalties, or patents filed, received, or pending), are the following: None.

Funding/Support and role of the sponsor: None.

Appendix A. Supplementary data

Supplementary data associated with this article can be found, in the online version, at https://doi.org/10.1016/j.euf.2018.11.004.

References

[1] Wang L, Hricak H, Kattan MW, et al. Prediction of seminal vesicle invasion in prostate cancer: incremental value of adding endorectal MR imaging to the Kattan nomogram. Radiology 2007;242:182–8.
[2] Carver BS, Bianco FJ, Scardino PT, Eastham JA. Long-term outcome following radical prostatectomy in men with clinical stage T3 prostate cancer. J Urol 2006;176:564–8.
[3] McClure TD, Margolis DJA, Reiter RE, Sayre JW, Thomas MA. Use of MR imaging to determine preservation of the neurovascular bundles at robotic-assisted laparoscopic prostatectomy. Radiology 2012;262:874–83.
[4] Ward JF, Slezak JM, Blute ML, Bergstralh EJ, Zincke H. Radical prostatectomy for clinically advanced (cT3) prostate cancer since the advent of prostate-specific antigen testing: 15-year outcome. BJU Int 2005;95:751–6.
[5] Partin AW, Kattan MW, Subong ENP, et al. Combination of prostate-specific antigen, clinical stage, and Gleason score to predict pathological stage of localized prostate cancer: a multi-institutional update. J Am Med Assoc 1997;277:1445–51.
[6] Steuber T, Graefen M, Haese A, et al. Validation of a nomogram for prediction of side specific extracapsular extension at radical prostatectomy. J Urol 2006;175:939–44, discussion 944.
[7] Ohori M, Kattan MW, Koh H, et al. Predicting the presence and side of extracapsular extension: a nomogram for staging prostate cancer. J Urol 2004;171:1844–9.
[8] Graefen M, Haese A, Pichlmeier U, et al. A validated strategy for side specific prediction of organ confined prostate cancer: a tool to select for nerve sparing radical prostatectomy. J Urol 2001;165:857–63.
[9] Barentsz JO, Richenberg J, Clements R, et al. ESUR prostate MR guidelines 2012. Eur Radiol 2012;22:746–57.

[10] Baco E, Ukimura O, Rud E, et al. Magnetic resonance imaging–transrectal ultrasound image-fusion biopsies accurately characterize the index tumor: correlation with step-sectioned radical prostatectomy specimens in 135 patients. Eur Urol 2015;67:787–94.
[11] Radtke JP, Schwab C, Wolf MB, et al. Multiparametric magnetic resonance imaging (MRI) and MRI–transrectal ultrasound fusion biopsy for index tumor detection: correlation with radical prostatectomy specimen. Eur Urol 2016;70:846–53.
[12] Morlacco A, Sharma V, Viers BR, et al. The incremental role of magnetic resonance imaging for prostate cancer staging before radical prostatectomy. Eur Urol 2017;71:701–4.
[13] de Rooij M, Hamoen EHJ, Witjes JA, Barentsz JO, Rovers MM. Accuracy of magnetic resonance imaging for local staging of prostate cancer: a diagnostic meta-analysis. Eur Urol 2016;70:233–45.
[14] Boesen L, Chabanova E, Løgager V, Balslev I, Mikines K, Thomsen HS. Prostate cancer staging with extracapsular extension risk scoring using multiparametric MRI: a correlation with histopathology. Eur Radiol 2015;25:1776–85.
[15] Radtke JP, Hadaschik BA, Wolf MB, et al. The impact of magnetic resonance imaging on prediction of extraprostatic extension and prostatectomy outcome in patients with low-, intermediate- and high-risk prostate cancer: try to find a standard. J Endourol 2015;29:1396–405.
[16] Somford DM, Hamoen EH, Fütterer JJ, et al. The predictive value of endorectal 3 Tesla multiparametric magnetic resonance imaging for extraprostatic extension in patients with low, intermediate and high risk prostate cancer. J Urol 2013;190:1728–34.
[17] Rayn KN, Bloom JB, Gold SA, et al. Added value of multiparametric magnetic resonance imaging to clinical nomograms in predicting adverse pathology in prostate cancer. J Urol 2018;200:1041–7.
[18] Radtke JP, Kuru TH, Boxler S, et al. Comparative analysis of transperineal template saturation prostate biopsy versus magnetic resonance imaging targeted biopsy with magnetic resonance imaging-ultrasound fusion guidance. J Urol 2015;193:87–94.
[19] Weinreb JC, Barentsz JO, Choyke PL, et al. PI-RADS prostate imaging–reporting and data system: 2015, version 2. Eur Urol 2016;69:16–40.
[20] Vuong QH. Likelihood ratio tests for model selection and non-nested hypotheses. Econometrica 1989;57:307–33.
[21] Martini A, Gupta A, Lewis SC, et al. Development and internal validation of a side-specific, multiparametric magnetic resonance imaging-based nomogram for the prediction of extracapsular extension of prostate cancer. BJU Int 2018. http://dx.doi.org/10.1111/bju.14353, [Epub ahead of print]..
[22] Epstein JI, Zelefsky MJ, Sjoberg DD, et al. A contemporary prostate cancer grading system: a validated alternative to the Gleason score. Eur Urol 2016;69:428–35.
[23] Cole AI, Morgan TM, Spratt DE, et al. Prognostic value of percent Gleason grade 4 at prostate biopsy in predicting prostatectomy pathology and recurrence. J Urol 2016;196:405–11.
[24] Horiguchi A, Nakashima J, Horiguchi Y, et al. Prediction of extraprostatic cancer by prostate specific antigen density, endorectal MRI, and biopsy Gleason score in clinically localized prostate cancer. Prostate 2003;56:23–9.
[25] Billing A, Buchner A, Stief C, Roosen A. Preoperative mp-MRI of the prostate provides little information about staging of prostate carcinoma in daily clinical practice. World J Urol 2015;33:923–8.
[26] Tay KJ, Gupta RT, Brown AF, Silverman RK, Polascik TJ. Defining the incremental utility of prostate multiparametric magnetic resonance imaging at standard and specialized read in predicting extracapsular extension of prostate cancer. Eur Urol 2016;70:211–3.
[27] Wibmer A, Vargas HA, Donahue TF, et al. Diagnosis of extracapsular extension of prostate cancer on prostate MRI: impact of second-opinion readings by subspecialized genitourinary oncologic radiologists. AJR Am J Roentgenol 2015;205:73–8.
[28] Baco E, Rud E, Vlatkovic L, et al. Predictive value of magnetic resonance imaging determined tumor contact length for extracapsular extension of prostate cancer. J Urol 2014;193:466–72.
[29] Petralia G, Musi G, Padhani A, et al. Robot-assisted radical prostatectomy: multiparametric MR imaging–directed intraoperative frozen-section analysis to reduce the rate of positive surgical margins. Radiology 2015;274:434–44.
[30] Schlomm T, Tennstedt P, Huxhold C, et al. Neurovascular structure-adjacent frozen-section examination (NeuroSAFE) increases nerve-sparing frequency and reduces positive surgical margins in open and robot-assisted laparoscopic radical prostatectomy: experience after 11 069 consecutive patients. Eur Urol 2012;62:333–40.
[31] Rosenkrantz AB, Ginocchio LA, Cornfeld D, et al. Interobserver reproducibility of the PI-RADS version 2 lexicon: a multicenter study of six experienced prostate radiologists. Radiology 2016;280:793–804.
[32] Faria R, Soares MO, Spackman E, et al. Optimising the diagnosis of prostate cancer in the era of multiparametric magnetic resonance imaging: a cost-effectiveness analysis based on the prostate MR imaging study (PROMIS). Eur Urol 2018;73:23–30.